Geological Quarterly, 2024, 68: 13
DOI: http://dx.doi.org/10.7306/gq.1742

Baltoscandian Ordovician and Silurian brachiopod carbon and oxygen stable isotope trends: implications for palaeoenvironmental and palaeotemperature changes

Bilal GUL[1,] *, Leho AINSAAR[1] and Tõnu MEIDLA[1]

[1] University of Tartu, Department of Geology, Ravila 14a, 50411 Tartu, Estonia; ORCID: 0009-0007-3198-4101 [B.G.], 0000-0002-0347-9577 [L.A.], 0000-0002-3822-4291 [T.M.]

Gul, B., Ainsaar, L., Meidla, T., 2024. Baltoscandian Ordovician and Silurian brachiopod carbon and oxygen stable isotope trends: implications for palaeoenvironmental and palaeotemperature changes. Geological Quarterly, 2024, 68: 13; https://doi.org/10.7306/gq.1742

Oxygen isotope palaeotemperature studies of Paleozoic limestones are based mainly on brachiopod shell material which is resistant to diagenesis and generally precipitated in oxygen isotopic equilibrium with ambient sea water. Here we present brachiopod C and O stable isotopic data from the Baltoscandian Ordovician-Silurian succession, and evaluate palaeotemperature and palaeoenvironmental variability during deposition of the Estonian Shelf facies. As the region has not been influenced significantly by tectonic events or deep burial diagenesis, the carbonate rocks and fossils are well-preserved in most of the locations studied. $\delta^{18}O$ values for the Ordovician and Silurian carbonates and brachiopods range between ~–7 and 0‰. High $\delta^{18}O$ values, locally accompanied by higher $\delta^{13}C$ values, correspond to cooling if the isotope signal reflects the original oxygen isotopic composition in sea water and *vice versa*. Several Ordovician-Silurian $\delta^{13}C_{brac}$ excursions identified on the Estonian Shelf reflect global palaeoenvironmental history and events, being synchronous with previously documented excursions in the bulk carbonate stable isotopic curves. Combining the published and new $\delta^{13}C_{brac}$ and $\delta^{18}O_{brac}$ data allows us to address chemostratigraphic correlation of the interval from Lower Ordovician (Floian) up to the topmost Silurian (Přídolí). The $\delta^{18}O_{brac}$ data corroborate warmer temperatures during Early Ordovician (Floian-Dapingian) and a cooling trend into the Mid-Ordovician documented by previous studies in different palaeobasins. The Hirnatian isotopic carbon excursion (HICE) episode reveals the minimum temperature in this interval and the post-HICE data suggest a rising temperature trend. Another temperature minimum is evident in the strata reflecting the Ireviken Event (Sheinwoodian). Our study shows that brachiopod $\delta^{18}O$ values from the Ordovician-Silurian carbonates may tentatively be interpreted as reflecting major temperature trends.

Key words: stable carbon and oxygen isotopes, sea level, brachiopods, palaeotemperature, Ordovician, Silurian.

INTRODUCTION

Stable oxygen isotopes in biogenic materials are precipitated in equilibrium with ambient waters and provide valuable information about water temperature, precipitation, and chemical composition. Although stable carbon isotopic curves obtained from biogenic material generally reflect the change in the marine carbon influx, the source material of primary data may not be so strongly temperature-dependent (Epstein et al., 1951; Brenchley et al., 2003; Shields et al., 2003). The challenge to reliable oxygen isotope palaeothermometry of the Ordovician and Silurian systems lies in the ambiguity of the stable oxygen isotope composition of the ambient sea water and the diagenesis of fossils (Grossman, 2012). Brachiopods are considered to be one of the most suitable groups for stable isotopic studies of the Paleozoic Era as their low-Mg calcite shells are more resilient to diagenesis than high-Mg calcite shells, thus retaining the primary isotopic signals much better (Azmy et al., 1998). Relatively good preservation of the Paleozoic strata due to limited post-depositional tectonics and insignificant thermal alteration makes Baltoscandia an ideal study area and a key region for global Ordovician-Silurian chemostratigraphic correlation (Ainsaar et al., 2010).

During the Ordovician and Silurian periods, dramatic climatic changes took place. The Ordovician period was characterized by a substantial increase in marine biodiversity designated as the Great Ordovician Biodiversification Event (GOBE), that brought along the rise of a complex Paleozoic marine ecosystem. As background, rapid sea level fluctuations and numerous positive carbon isotope ($\delta^{13}C$) excursions have been documented. The Ordovician Period was terminated by a major marine extinction event (termed the Hirnantian event), the loss of 85% of marine animals (Sheehan, 2001; Trotter et al., 2008; Bartlett et al., 2018), followed by a slow biotic recovery (Munnecke et al., 2010). The extinction is mostly regarded as the result of an abrupt change in climate (Hirnantian glaciation) that caused ice-sheet formation over the most of Gondwana and a

* Corresponding author, e-mail: bilal.gul@ut.ee
Received: August 10, 2023; accepted February 6, 2024; first published online: April 20, 2024

global sea level fall; regions that were previously submerged marine shelf thus became subaerial, exposing $\delta^{13}C$-enriched carbonates (Brenchley et al., 2001; Trotter et al., 2008).

The beginning and duration of the Late Ordovician mass extinction (LOME), as well as its possible triggers and mechanisms, have been hotly debated in the recent publications (Hammarlund et al., 2012; Bond and Grasby, 2020; Zhang et al., 2022 and references therein). Several papers have also questioned the direct relationships between the LOME and the Hirnantian glaciation (Bond and Grasby, 2020; Hints et al., 2023 and references therein).

During the Darriwilian, substantial transformations occurred within Ordovician ecosystems, marked by a gradual cooling process that led to a significant decrease in sea-surface water temperatures at low latitudes, comparable to recent equatorial regions (Trotter et al., 2008). Recent insights indicate that the transition from a greenhouse to an icehouse climate might have taken place considerably earlier than previously suggested and that Darriwilian continental ice sheets influenced global sea levels (Rasmussen et al., 2016). Based on the Guttenberg isotopic carbon excursion (GICE), this has been historically interpreted as evidence of a prolonged Late Ordovician glaciation, commencing during the latest Sandbian-early Katian interval (Saltzman and Young, 2005; Goldman et al., 2020). A brief cooling phase, indicated by $\delta^{18}O$ values, has been linked to the GICE and tentatively linked to the onset of Ordovician icehouse conditions (Rosenau et al., 2012). However, a thorough investigation of both previous and recently collected conodont $\delta^{18}O$ data from Laurentia, spanning the Sandbian-Katian boundary through the GICE interval, demonstrates an inconsistent warming trend throughout the late Sandbian–early Katian, and shows no evidence of cooling (Quinton et al., 2018). A $\delta^{18}O_{phos}$ study of the Sandbian-Katian interval suggests a slight rise in temperature and a gradual cooling during the late Katian, followed by an abrupt decline in temperature during the latest Ordovician (Hirnantian) and the glacially driven mass extinction (Buggisch et al., 2010).

Following the late Ordovician–early Silurian glaciation, multiple small-scale climate cycles demonstrate a general warming trend until the mid-Llandovery (early-mid Telychian), then a progressive cooling trend until the late Llandovery (Grossman and Joachimski, 2020). Wenlock $\delta^{18}O_{phos}$ excursions coincided closely with the Ireviken biotic event (Lehnert et al., 2010; Trotter et al., 2016).

General understanding on the environmental history of Baltica, however, has been based on palaeogeographic reconstructions (Goldman et al., 2020; Meidla et al., 2023) which document continental drift of Baltica from southern latitudes to the proximity of equator during the Middle-Late Ordovician. Because of that, a gradual warming throughout the Ordovician and Silurian, with a possible brief temperature decline during the latest Ordovician glaciation, was proposed for Baltica in many publications of the past decades (e.g., Nestor and Einasto, 1997 and references therein) while actual temperature data from the region were missing. The results of a pilot study on pre-Hirnantian palaeotemperature changes based on $\delta^{18}O_{phos}$ (Männik et al., 2021) has recently questioned this scenario and makes a palaeotemperature reconstruction from different proxies particularly relevant in this area.

This study elaborates a tentative palaeotemperature curve based on new and published $\delta^{18}O$ data from brachiopod shells spanning from the Lower Ordovician (Floian) up to Přidoli Epoch in the Baltoscandian region.

GEOLOGICAL SETTING

During the Paleozoic, present-day northern Europe was covered by a widespread epeiric sea characterized by slow but continuous carbonate deposition throughout the Middle to Late Ordovician and the Silurian (Nestor and Einasto, 1997). On the basis of the pattern of rock and faunal distribution along the facies gradient, from shallow-water to deeper basinal environments, three main facies belts have been distinguished in the Baltoscandian basin (Fig. 1). The North Estonian Shelf and Lithuanian Shelf Facies Belt (the Estonian and Lithuanian basins of Harris et al., 2004) were the shallowest parts of the palaeobasin and were characterized mainly by carbonate deposits. The Central Baltoscandian Facies Belt (the Scandinavian Basin of Harris et al., 2004) stretched from present-day southern Estonia to Latvia and Sweden, representing deeper shelf conditions and being characterized by widespread argillaceous limestones and mudstones. The Scanian Facies Belt in southern Scandinavia (the Scanian Basin of Harris et al., 2004) covers the deepest part of the basin characterized by wide distribution of graptolitic black shales (Kaljo et al., 2007).

The general stratigraphy of the Ordovician and Silurian systems in Baltoscandia is shown in Figure 2. Regional stages are the primary unit in Estonian Paleozoic chronostratigraphic classification, defined historically on the basis of fauna and characteristic lithology, rather than by boundaries (Männik et al., 2021; Hints et al., 2023: Meidla et al., 2023 and references therein).

The Early Ordovician strata comprise a relatively thin succession of clastic deposits. Sandstones, mudstones and clays of the Pakerort and Varangu regional stages are overlain by glauconitic sandstones and siltstones of the Hunneberg and Billingen regional stages. The Billingen Regional Stage marks the transition from siliciclastic to carbonate rocks (Meidla et al., 2014).

Throughout the early Paleozoic, the climatic conditions in Baltica were thought to have been influenced by gradual northwards drift, from high southern latitudes into subtropical and tropical zones. The depositional history is generally characterized as an Early Ordovician cold-water siliciclastic ramp environment (Tremadocian) replaced by a cool-water carbonate (glauconite-rich) ramp with an extremely low sedimentation rate (Floian). From the Darriwillian to Sandbian this evolved into a temperate carbonate ramp and subsequently into a tropical carbonate shelf during the Katian to Hirnantian transition (Dronov and Rozhnov, 2007). Carbonate production and sedimentation rate on the carbonate shelf increased as a result of drift-induced climate change throughout the Middle and Late Ordovician. This all was happening, though, against a background of global cooling as shown by a progressive decline in sea water temperatures during the Ordovician, with glacials and interglacials possibly starting in the late Middle Ordovician (Trotter et al., 2008; Torsvik and Cocks, 2016; Rasmussen et al., 2016). The Silurian succession represented by shallow-shelf limestones and dolomites is rich in shelly faunas. Silurian deeper-water facies from southwestern Estonia and Latvia are dominated by argillaceous rocks, ranging from calcareous marlstones to black shales. During the Silurian Period, the Baltica continent was located in equatorial latitudes and drifted northwards (Melchin and Holmden, 2006). The pericontinental Baltic palaeobasin, embracing the territory of Estonia, was characterized by a wide range of tropical shelf environments and diverse biotas.

Fig. 1. Locality map showing the outcrops of Ordovician and Silurian rocks in the Baltic region and schematic configuration of the Baltoscandian basin (modified from Harris et al., 2004)

The present study addresses the interval from the topmost Lower Ordovician (Floian) up to the Přidoli, beginning with the first Ordovician carbonates. In northern and central Estonia, the upper Floian and Dapingian are represented by the Toila Formation, of locally dolomitized glauconitic limestone (Nestor and Einasto, 1997). The lower Darriwilian comprises the Pakri Formation in NW Estonia which is represented by sandy limestone supplemented with kukersite kerogen and calcareous sandstone (Meidla et al., 2023). The Mid-Darriwilian-Mid-Sandbian interval is not represented in the brachiopod dataset.

The Middle and Upper Ordovician comprises various cool-water carbonates that are locally dolomitized and include thin volcanic interbeds (K-bentonites) at several levels. The mid-Katian comprises a package of intercalating micritic and argillaceous bioclastic limestones (Cocks and Torsvik, 2005). The Upper Ordovician reflects a change from cool water to tropical carbonate sedimentation (Nestor and Einasto, 1997). The basal Hirnantian is represented by the Ärina Formation in north Estonia, comprising poorly fossiliferous dolomites overlain by a complex reef succession (reef bodies, fore-reef grainstones and back-reef bituminous carbonates) and capped by oolitic and/or sandy limestone barren of fossils (Kaljo et al., 2001).

The base of the Silurian is fixed in the Dobs Linn section at the FAD of *Akidograptus ascensus* (Rong et al., 2008). Because of the scarcity of graptolites in the uppermost Ordovician and lowermost Silurian transition interval in Estonia, the lower boundary of the Silurian is tentatively drawn within the Varbola Formation, based on chemostratigraphic evidence (see Meidla et al., 2020 and references therein).

The Rhuddanian Stage begins within a unit of nodular argillaceous limestone (packstone; Varbola Formation) overlain by massive coquinoid limestones with abundant *Borealis borealis* brachiopods of the Tamsalu Formation (Ainsaar et al., 2015). The topmost Rhuddanian to Aeronian consists of cyclical alternation of limestones and lagoonal argillaceous dolomites, marlstones, and micritic and bioclastic limestones. The boundary between the Llandovery and Wenlock is drawn within the Jaani Formation (Fig. 2B) which consists mainly of marls and mudstones grading into limestones in its upper part (Männik, 2014). In southern Estonia, the equivalent strata are represented by grey mudstone with graptolites. The overlying Sheinwoodian-Homerian comprises bioclastic limestones and dolomites with abundant bioherms grading eastwards into the dolomitised reef succession of the Muhu Formation. The upper Wenlock and

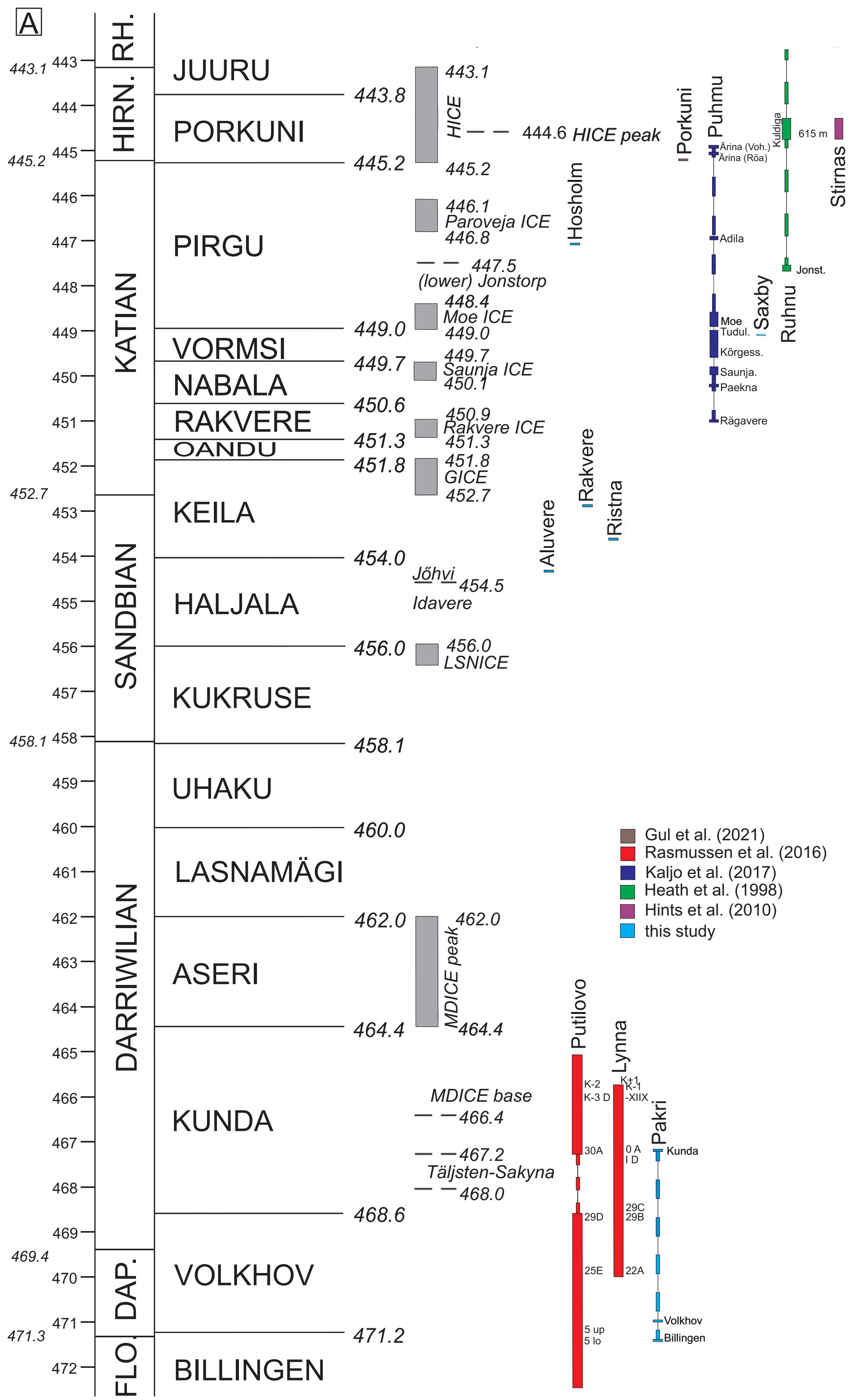

Fig. 2A, B – global Ordovician and Silurian stratigraphy and Baltoscandian regional stages (RS), modified from (Gradstein et al., 2020)

Vertical columns show intervals studied and referred to the vertical bars that represent outcrops and drill cores studied

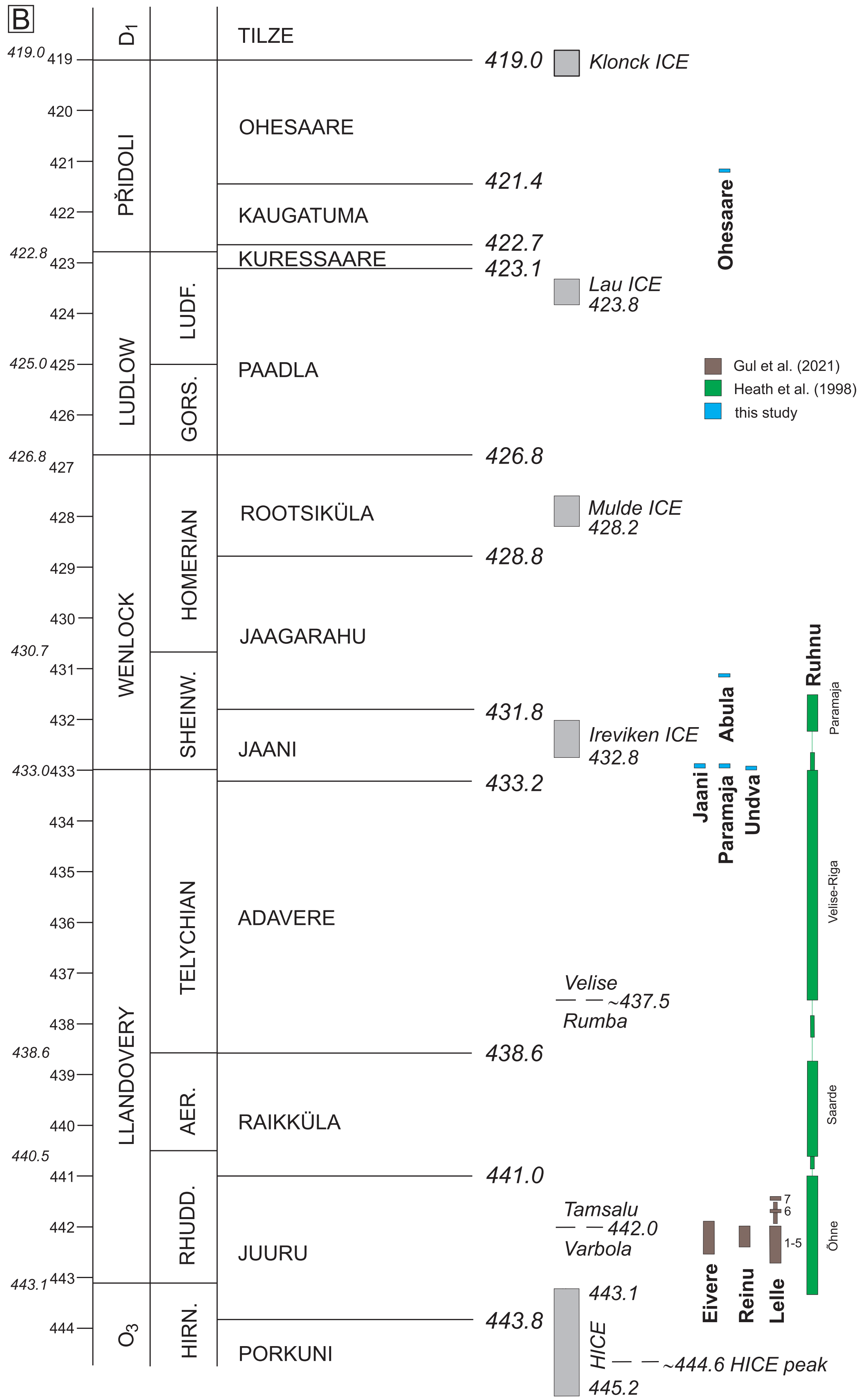
B
D1
TILZE
419.0
Klonck ICE
PŘIDOLI
OHESAARE
421.4
KAUGATUMA
422.7
KURESSAARE
423.1
Lau ICE 423.8
Ohesaare
LUDLOW
LUDF.
GORS.
PAADLA
Gul et al. (2021)
Heath et al. (1998)
this study
426.8
WENLOCK
HOMERIAN
ROOTSIKÜLA
Mulde ICE 428.2
428.8
JAAGARAHU
SHEINW.
431.8
JAANI
Ireviken ICE 432.8
Abula
Ruhnu
Paramaja
433.2
Jaani
Paramaja
Undva
LLANDOVERY
TELYCHIAN
ADAVERE
Velise-Riga
Velise
~437.5
Rumba
438.6
AER.
RAIKKÜLA
Saarde
441.0
RHUDD.
JUURU
Tamsalu
442.0
Varbola
Õhne
Eivere
Reinu
Lelle
O3
HIRN.
PORKUNI
443.8
443.1
HICE
~444.6 HICE peak
445.2

Fig. 2B

Ludlow are poorly fossiliferous, because of extensively developed very marginal-marine and lagoonal facies, and are therefore not represented in the data set. The Přidoli interval is represented in this study by the Ohesaare Formation, thin-bedded bioclast-rich limestones and marls. All these rocks contain well-preserved fossils, with brachiopods being common.

MATERIAL AND METHODS

A total of 62 brachiopod samples were collected for this study from the 12 exposures in Estonia (Ohesaare, Abula, Jaani, Paramaja, Undva, Porkuni, Hosholm, Saxby, Rakvere, Ristna, Aluvere and Pakri; Fig. 1) irregularly spanning the Middle Ordovician to Přidoli interval. The new material covers mainly the Katian-Sheinwoodian interval and some Dapingian and Přidoli units. Previously published brachiopod isotopic data was used for comparison and for filling in the stratigraphic intervals not covered by the newly collected material (Heath et al., 1988; Hints et al., 2010; Rasmussen et al., 2016; Kaljo et al., 2017; Gul et al., 2021; see supplementary online data: https://dx.doi.org/10.23673/re-351). Brachiopods collected at exposures and from borehole cores were carefully removed from the limestone matrix and cleaned. The state of the shells and fragments did not generally allow identification of specific families or genera due to their poor condition. For stable isotope analyses, brachiopod shell powder was obtained by micro-drilling, avoiding cement and matrix material. The powdered material was analysed for stable isotopes (oxygen and carbon) using a *Thermo Scientific Delta V Advance* continuous flow isotope ratio mass spectrometer at the Department of Geology, University of Tartu. Delta V advantage (continuous flow) + GasBench II samples were dissolved (reaction time >8 hours) in H_3PO_4 (99%) at 25°C. About 0.5 mg of the powdered sample was used. The results are reported as δ notation in per mil relative to Peedee belemnite (VPDB) for both oxygen and carbon, and reproducibility of the results is generally better than ±0.1 and ±0.2‰ for carbon and oxygen (respectively). The international laboratory standards (from IAEA) IAEA-60, NBS 18 and LSVEC were used. For palaeotemperature estimates we calculated temperatures from $\delta^{18}O_{brac}$ values using the formula $T°C = 17.3750–4.2535 (\delta c–\delta w) +0.1473 (\delta c–\delta w)^2$, assuming possible preservation of an original marine carbonate isotopic composition formed in sea water with $\delta^{18}O$ value –1‰ (Brand et al., 2019). Trace-element analysis (Ca, Sr, Mg, Mn, Fe) was obtained from 12 brachiopod samples by electron microprobe analysis operating at voltage of 20 kV, beam current 0.015 mA, and 13 mm beam diameter (detection limits for Sr = 200 ppm, Mg = 100 ppm, Mn = 200 ppm, Fe = 200 ppm), in order to evaluate the preservation of the material and reliability of the stable isotopic signal.

RESULTS

CARBON AND OXYGEN ISOTOPES

The $\delta^{18}O$ and $\delta^{13}C$ values for Ordovician and Silurian brachiopods used in this study range between ~–7 to 0‰ and –2.6 to +7.6‰ respectively (Figs. 3 and 4). The individual values are widely dispersed across the succession but the principal trends are obvious and can be discussed based on the averaged curve.

The carbonate rocks and fossils examined in the earlier study show excellent preservation across most of the localities studied in Estonia. This is due to low tectonic activity and limited burial diagenesis in the area (Azmy et al., 1998). The evaluation of diagenetic changes in carbonate isotopic composition can be done by analysing the $\delta^{13}C$–$\delta^{18}O$ cross-plot of brachiopod shell material. According to Jacobsen and Kaufman (1999), the relationship between $\delta^{13}C$ and $\delta^{18}O$ values in this plot indicates the extent of meteoric diagenesis. However, the cross-plot of carbon and oxygen isotopic data of randomly selected samples in our study shows no correlation between the $\delta^{13}C$ and $\delta^{18}O$ values (R2 = 0.0072, as shown in Fig. 5). The values are closely clustered without any extreme negative points on either axis, which suggests that the preservation of the shells is relatively good. Nevertheless, it still cannot be completely ruled out that some secondary influence may have affected the primary signal in some samples.

Brachiopod shells have been widely used also to estimate diagenetic alteration, with strontium (Sr) and manganese (Mn) abundance ratio serving as key indicators (Brand and Veizer, 1980). Figure 6 illustrates the results obtained from 10 brachiopod shells that successfully passed the petrographic screening tests. The Sr abundances range from 359 to 2159 ppm (mean: 898 ppm) whilst concentrations as low as 200 ppm have been documented for modern brachiopods (Veizer et al., 1999; Immenhauser et al., 2002). The manganese abundances range from below the detection limit up to 58 ppm (mean: 28 ppm). These values align with the range observed in modern low-Mg calcite shells (Veizer et al., 1999), showing that their retained values are close to their primary isotopic composition.

The Floian-Darriwilian $\delta^{13}C_{brac}$ values are characterized by an increasing-upwards trend on average from –1 to 0‰ (Fig. 3). The Sandbian-Katian $\delta^{13}C_{brac}$ values vary generally between 1 and 2‰, but the resolution is too low to recognize the well-known isotopic excursions revealed in the bulk carbon data (e.g., Ainsaar et al., 2020). The Ordovician succession is terminated by a sharp increase in the $\delta^{13}C_{brac}$ values up to +5–7‰ in the Hirnantian Stage (the HICE peak). The falling limb of the HICE curve is marked by $\delta^{13}C_{brac}$ values returning to ~–1 to 0‰ in the topmost Ordovician.

The $\delta^{18}O_{brac}$ values in the Ordovician Baltoscandian succession generally increase from the Floian to the Hirnantian. These values rise gradually from –6 to –5‰ in the Floian-Darriwilian interval but are more scattered in the Sandbian-Katian interval (between –6 and –3‰), without obvious trends or peaks (Fig. 4).

The Hirnantian $\delta^{18}O$ averaged brachiopod values show an abrupt increase from roughly –4 to –2‰, with a maximum coinciding with the Hirnantian glaciation event (Fig. 4), before returning to the pre-shift plateau in the basal Llandovery beds. This abrupt fall in $\delta^{18}O_{brac}$ values marks a stratigraphic gap at the boundary of the Porkuni and Juuru regional stages in this area (Kaljo et al., 2001). The average $\delta^{18}O_{brac}$ values in the Silurian indicate a small rise in the upper Rhuddanian (Llandovery) followed by a continuous decline up to the Telychian-Sheinwoodian boundary, in the range of ~–5.5 to –4.5‰. Throughout the mid-Sheinwoodian, the average value of $\delta^{18}O_{brac}$ shows an increase up to –3.5‰. The $\delta^{18}O_{brac}$ values in the Přidoli are ~–6‰ (Fig. 4).

Secular trends in the $\delta^{13}C_{brac}$ values in the Silurian part of the succession may be divided into three intervals. A large

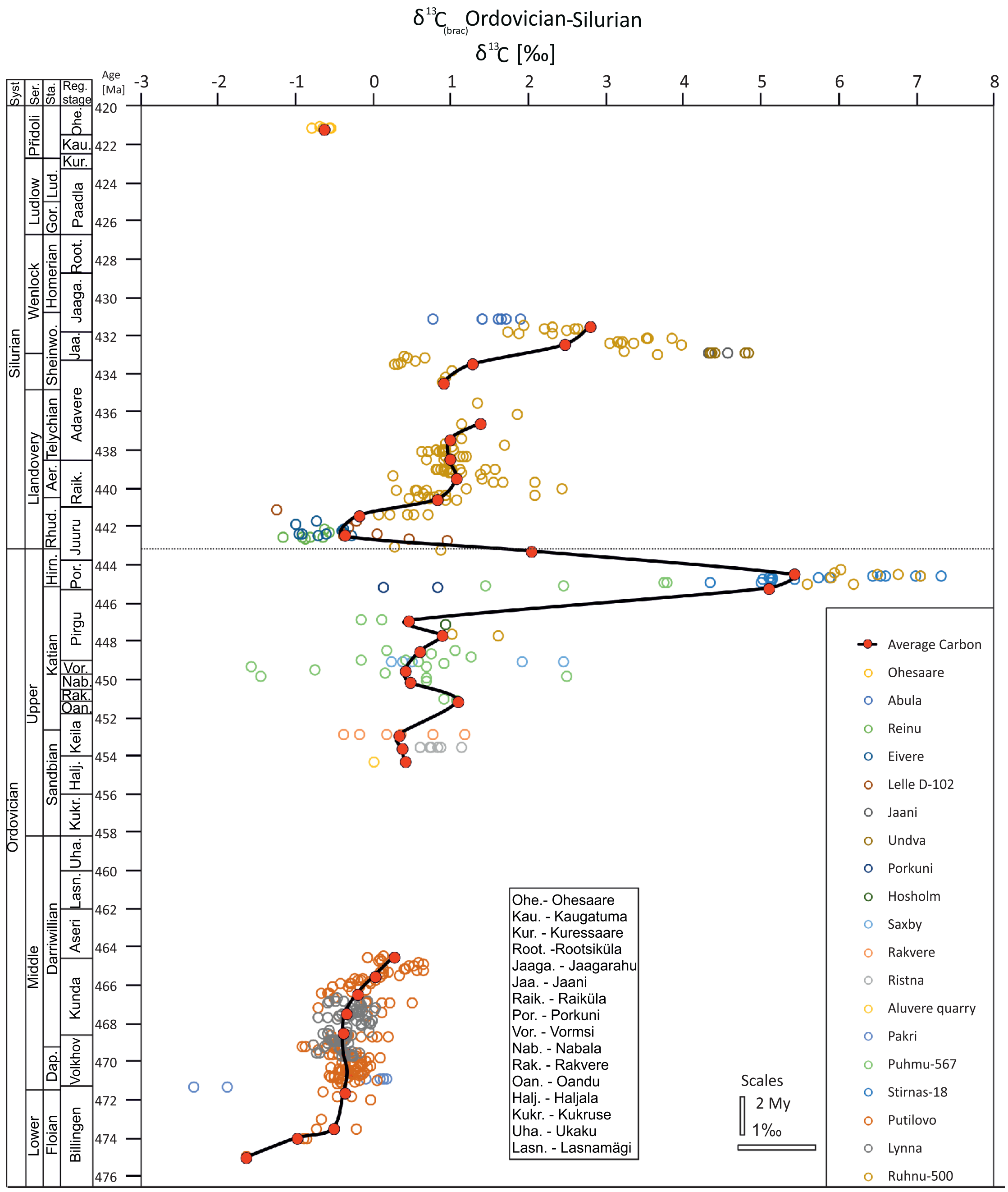

Fig. 3. Summary figure showing the carbon isotope (brachiopod) trend through the early Ordovician–late Silurian interval

The average curve comprises two-million-year segments with a centred moving average computed every 0.5 My

positive $\delta^{13}C$ shift is recorded throughout the early Silurian (Rhuddanian-Aeronian interval) where $\delta^{13}C$ values gradually decrease up to +1‰. The second, Aeronian-Telychian interval is characterized by stable values around +1‰. This is followed by a continuous increase in the $\delta^{13}C_{brac}$ values up to +3.5‰ in the Sheinwoodian interval, reflecting the global Ireviken Event (Munnecke et al., 2010). There is no brachiopod data in our dataset from Homerian to Ludfordian, partly due to wide distribution of marginal marine carbonates in the Baltic outcrops that are nearly barren of brachiopods. The $\delta^{13}C_{brac}$ values in the mid-Přidoli interval are the lowest for the Silurian in this region (–0.7‰; Fig. 3).

DISCUSSION

Over the last few decades, the Ordovician and Silurian succession in Baltoscandia has attracted researchers because of the many spectacular carbon isotope ($\delta^{13}C$) fluctuations that are well-documented, mainly in the bulk carbonate record (Kaljo et al., 2007; Ainsaar et al., 2010), and interpreted as markers of global or regional environmental changes but also extensively applied in regional stratigraphy. Numerous Ordovician positive $\delta^{13}C$ excursions in the Baltoscandian area have been described from different borehole core sections (Kaljo et al., 2007; Ainsaar

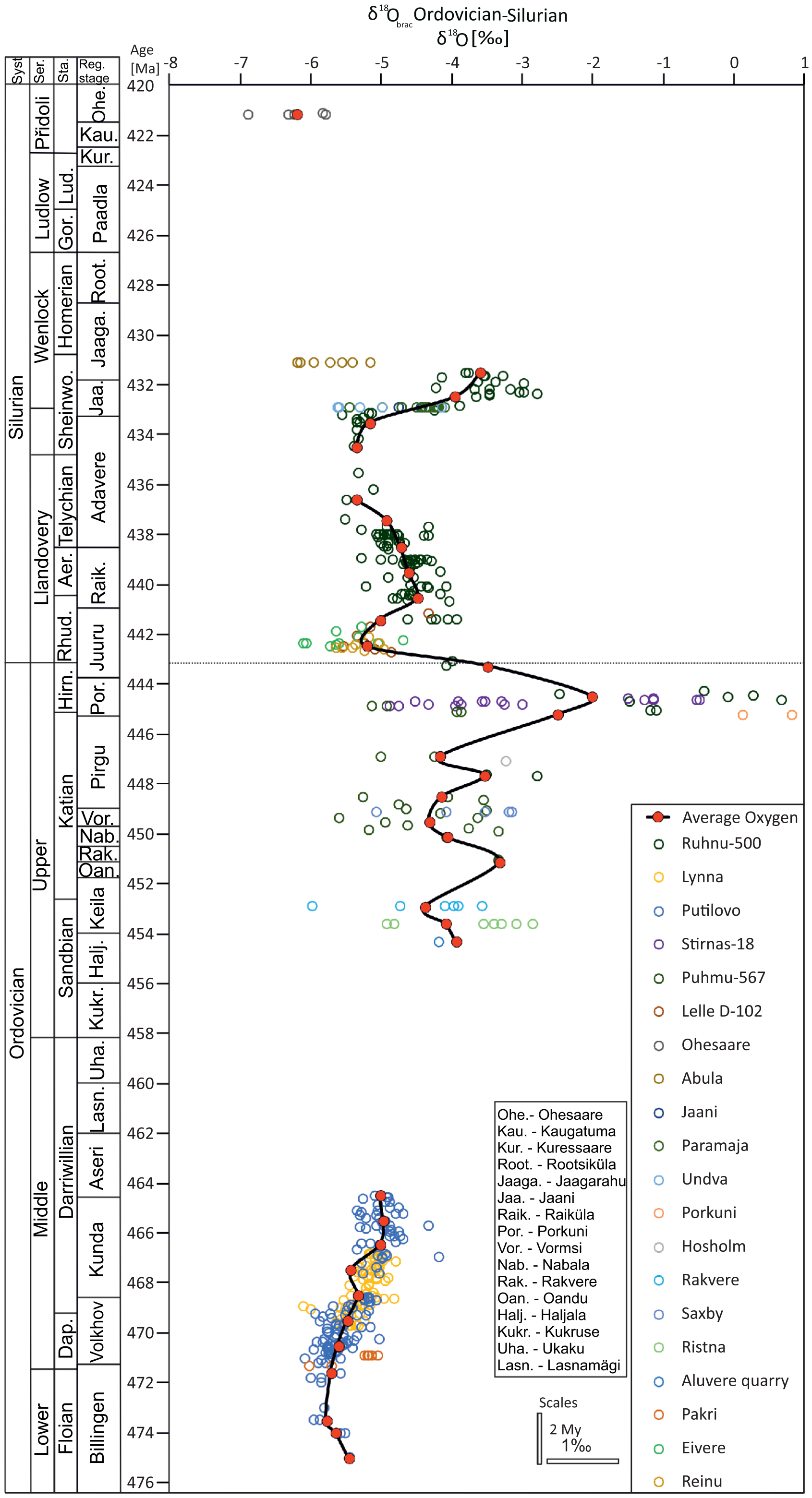

Fig. 4. Summary figure showing oxygen isotope compositions representing Baltica during the early Ordovician–late Silurian

The average curve comprises two-million-year centred segments with a moving average computed every 0.5 My

et al., 2010). Except for the HICE and the Ireviken Excursion, where the $\delta^{13}C$ values reached up to +7‰, all other excursions show $\delta^{13}C$ values of only between –1 and +2‰. The Ordovician $\delta^{13}C$ excursions can be correlated across the Baltoscandian palaeobasin and some of them across different palaeocontinents (the HICE and also the Ireviken Excursion). The carbon isotopic

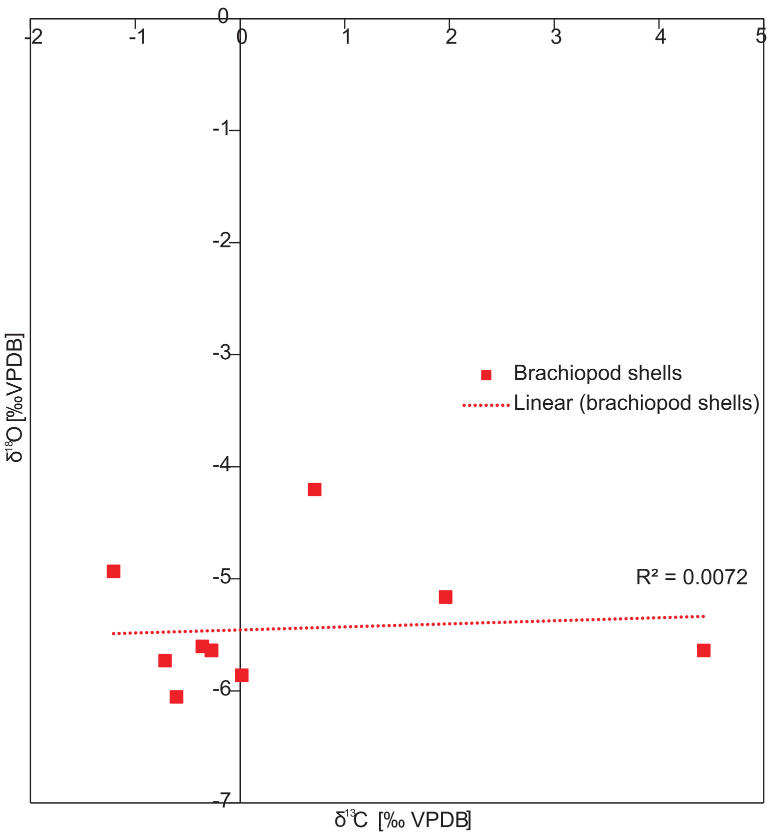

Fig. 5. Oxygen *versus* carbon isotopic composition measured from brachiopod shell material in the stratigraphic units studied

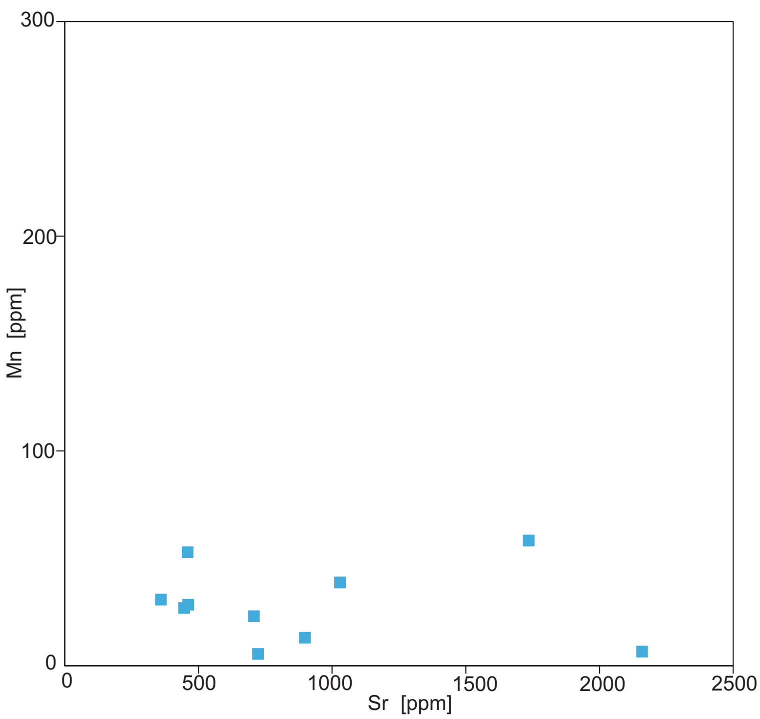

Fig. 6. Strontium and manganese abundances in the brachiopod shells used in this study

curve obtained based on brachiopod data is generally in agreement with the curves based on the bulk carbonate data (Heath et al., 1988; Hints et al., 2010; Männik et al., 2015; Rasmussen et al., 2016; Kaljo et al., 2017; Meidla et al., 2020; Gul et al., 2021), e.g. it contains the HICE and the Ireviken Excursion but insufficiently reflects smaller excursions as the frequency of brachiopod data is too low in these intervals. Deviations between the local and regional values of $\delta^{13}C_{brac}$ may be due to differences in depositional environments, tectonic regimes or the impact of diagenesis that may have affected the carbonate material.

The upwards rise of the $\delta^{13}C$ values in the Floian-Dapingian interval resembles that in an Ordovician dataset from south China (Edwards and Saltzman, 2014). The $\delta^{13}C_{brac}$ curve from the Darriwilian interval of Baltoscandian sections includes also the Mid-Darriwilian Carbon Isotope Excursion (MDICE) documented in the Baltoscandian area and worldwide in bulk carbonate data (Rasmussen et al., 2016). The well-known HICE $\delta^{13}C$ excursion has been reported globally from different palaeocontinents (Kaljo et al., 2001). The beginning and end of the HICE are not clearly defined. Within the *Metabolograptus extraordinarius* Zone, there is a gradual rise in $\delta^{13}C_{brac}$ values from the baseline, which corresponds to the time of glaciation in the early Hirnantian e.g. Wangjiawan North Section (Chen et al., 2006; Gorjan et al., 2012). Previous studies have recognized elevated $\delta^{13}C$ values in the Hirnantian in Estonia as well as in surrounding areas, corresponding to the HICE rising to a peak of up to +7‰ (Ainsaar et al., 2010; Gul et al., 2021). In more complete sections, the rising and falling limbs of the HICE curves display a similarity, i.e. both are gradual as observed in other Baltic sections studied using bulk rock samples, e.g. the Jurmala core (Ainsaar et al., 2010) as well as in coeval sections from several palaeocontinents e.g. south China (Chen et al., 2006; Ling et al., 2007), North America (Bergström et al., 2010) and elsewhere. The average $\delta^{13}C_{brac}$ curve is generally in agreement with the trends described and the lack of data points in the Porkuni-Juuru regional stage transition interval is noteworthy (Fig. 3), because of both the gap and the scarcity of fauna in this transition.

The potential of stable oxygen isotopic composition of sedimentary materials to reflect palaeotemperatures has long been recognized (Urey, 1947). Brachiopod shells have been widely used in palaeoclimatic studies of ancient carbonates because they are relatively resistant to diagenetic change. Most of the $\delta^{18}O_{brac}$ values in the current study fall in the interval of ~–7 to ~–0.5‰, implying some limited alteration by meteoric diagenesis. The current Baltoscandian Ordovician $\delta^{18}O$ dataset is consistent with the documented Ordovician pattern of increasing $\delta^{18}O$ values with decreasing age (Trotter et al., 2008; Grossman and Joachimski, 2020). The $\delta^{18}O_{brac}$ trends reflect multiple cooling events and deglaciation throughout the Ordovician-Silurian (Brenchley et al., 1994). The majority of the $\delta^{18}O_{brac}$

shifts are interpreted as resulting from sea surface water temperature changes as the critical factor that controls the oxygen isotope changes is temperature (Trotter et al., 2016). Still, as $\delta^{18}O$ variation can be influenced by several factors, including the isotopic composition of sea water, salinity, pH changes, source and composition of mud, vital effects and diagenetic alteration (Munnecke et al., 2010; Swart, 2015), the temperature estimates are considered tentative.

The brachiopod calcite temperature values in this study were calculated using the formula of Brand et al. (2019) assuming possible preservation of original marine carbonate isotopic composition formed in sea water with $\delta^{18}O$ value –1‰. The results obtained seem to be in a better agreement and are also closer to modern temperatures, compared to values revealed from bulk material in previous studies. If we would change the sea water $\delta^{18}O$ for the cooling episodes, then the change in 1‰ influences the temperature by up to 4°C. The curve could be slightly shifted at some intervals, if the sea water composition changed through time (e.g., during glacial episodes).

The temperature calculated from brachiopods from the Floian-Dapingian stages range from ~36 up to 43°C (Fig. 7). These values are clearly too high and seem to be unrealistic but this is a well-known problem. Some authors suggest that primary sea water $\delta^{18}O$ values might have been different during this time (Trotter et al., 2008). Although the Darriwilian sea water $\delta^{18}O$ values from Baltoscandia record imply that diagenesis

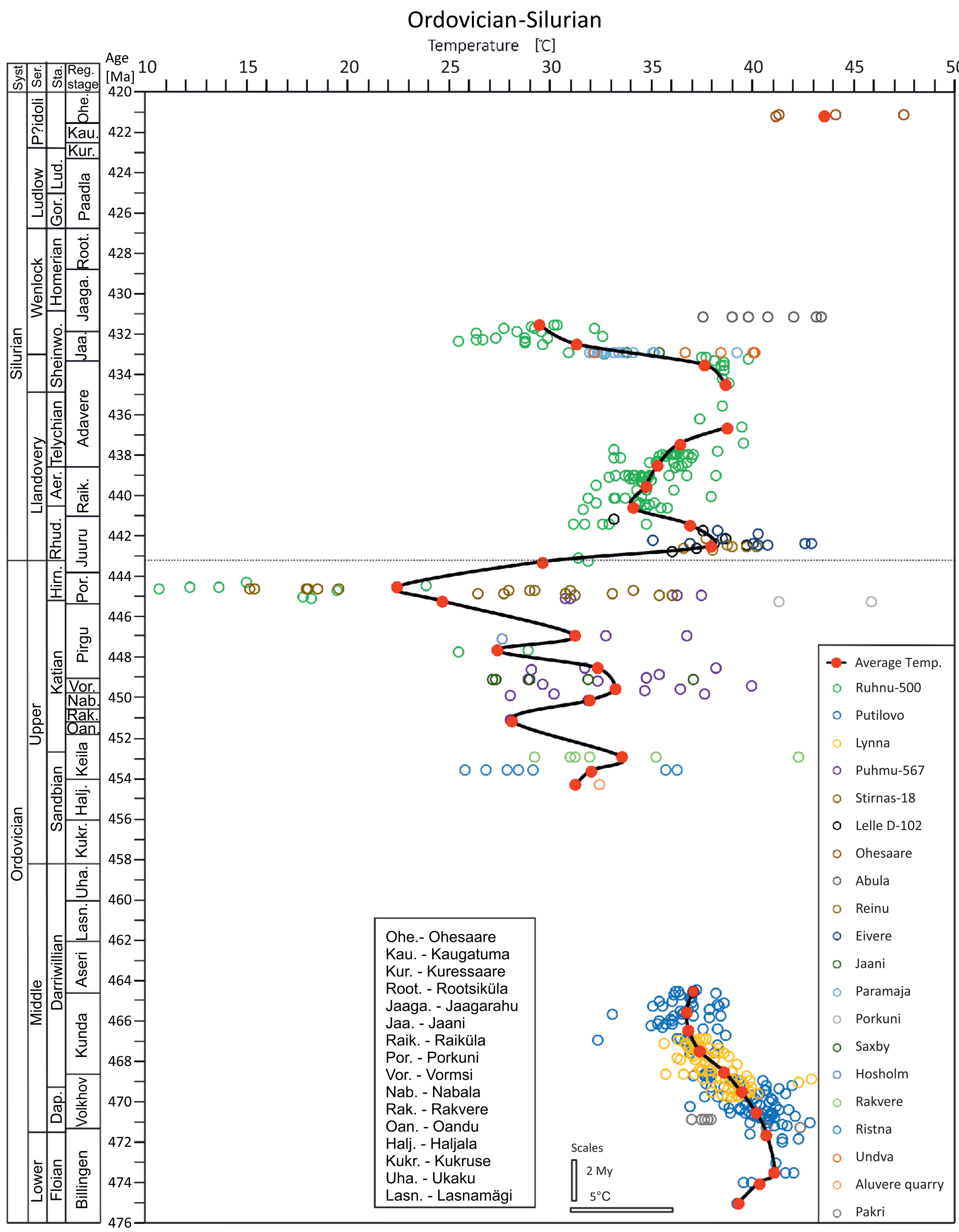

Fig. 7. Summary figure showing temperature based on oxygen isotope data

Temperatures are calculated from brachiopod data by the formula of Brand et al. (2019), assuming possible preservation of original marine carbonate isotopic composition formed in sea water of $\delta^{18}O$ value –1‰

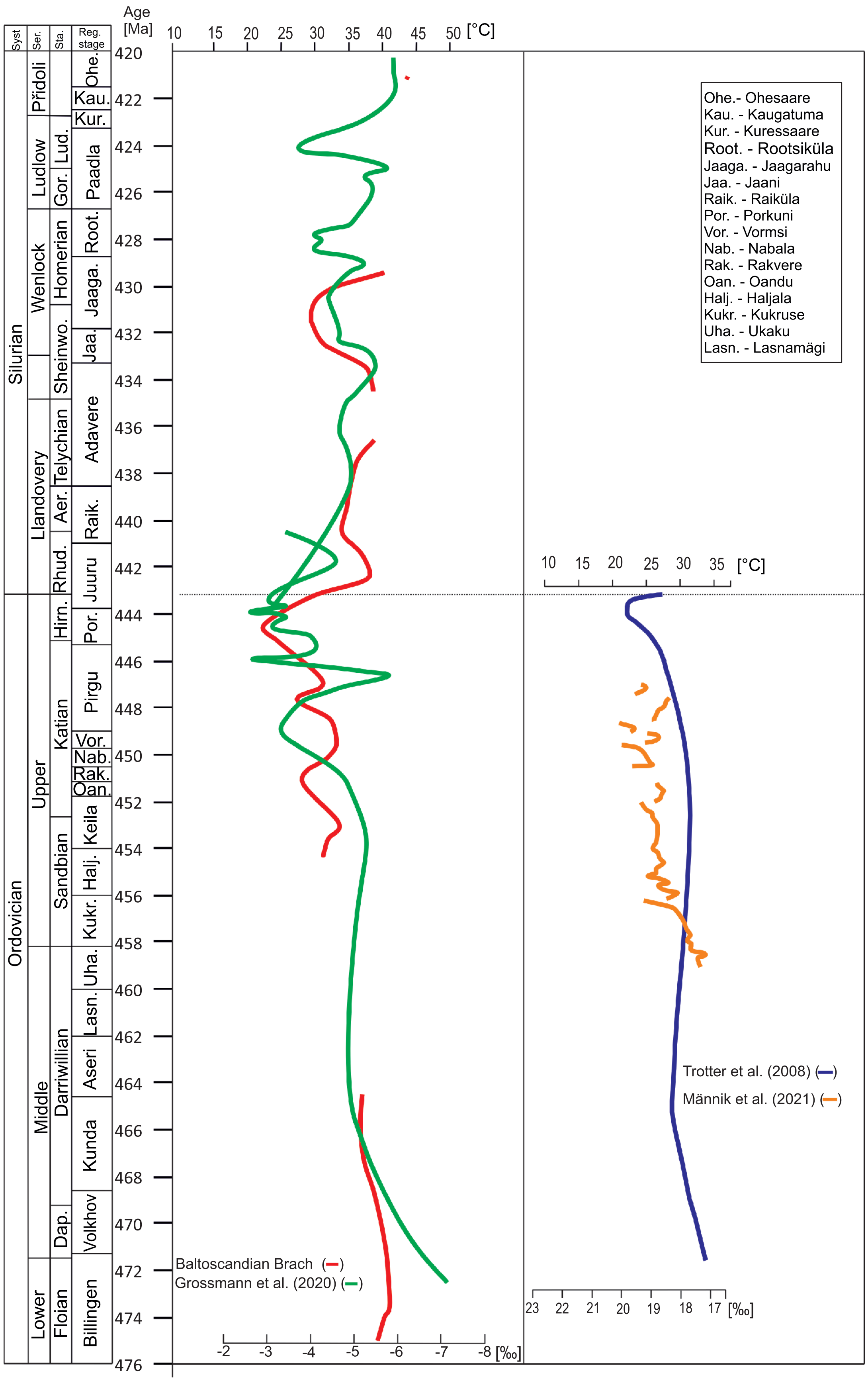

Fig. 8. Oxygen isotopic temperatures comparison of Ordovician-Silurian brachiopods (calcite) (Grossmann et al., 2020) and conodonts (phosphate) (from Trotter et al., 2008; Männik et al., 2021) assuming sea water $\delta^{18}O$ of –1‰

may have altered some of the primary $\delta^{18}O$ ratios, the well-preserved samples still reveal near-primary long-time $\delta^{18}O$ trends (Edward et al., 2022). A decline in the temperature values can be observed throughout the Darriwilian bringing the temperature values down into the interval of 32 and 38°C which is not far from modern tropical temperatures. Multiple temperature fluctuations ranging between ~25 and 37°C were calculated for the pre-Hirnantian Upper Ordovician brachiopods (Fig. 7). Even our maximum temperature of ~40°C, after adjusting for $\delta^{18}O$ seawater errors and an analytical of range ±3°C, is basically near the top limit of modern tropical temperatures.

With the start of HICE, the temperature drops to 27°C in the strata that correspond to low sea level and a global regression. Shortly after, there is an abrupt fall in temperature based on our averaged dataset to ~22°C which corresponds to the Hirnantian glaciation and this trend looks consistent with generally accepted Hirnantian scenarios (Brenchley et al., 2003; Trotter et al., 2008; Finnegan et al., 2011). However, the true temperature range is difficult to determine because of the ice-volume component which was clearly significant during the Hirnantian and had an impact on the sea water isotopic composition. The Hirnantian cooling phase coincided with a regional extinction (e.g., Meidla et al., 2020 and references therein).

The calculated post-HICE temperature shows a two-step rise. The temperatures calculated from brachiopods from the Rhuddanian mostly range between ~31 and 38°C, with few exceptions, possibly obtained from altered bioclasts (Gul et al., 2021). In the overlying strata (Aeronian and Telychian), temperatures range between ~30 and 38°C (Fig. 7), not far from modern tropical temperatures. The brachiopod calcite temperature values in the Sheinwoodian are distinctly lower, varying between ~25 and 38°C. The temperatures calculated for the Přidoli (Ohesaare) Age range between ~39 and 43°C, being slightly higher again in comparison to modern values. Our compiled data suggests a warming trend in the early Silurian (Llandovery), followed by a return to colder temperatures in the Sheinwoodian while a warmer climate is recorded in the Přidoli time (Grossman and Joachimski, 2020).

During the previous decade, Trotter et al. (2008) and Finnegan et al. (2011) reconstructed temperature trends for the Ordovician-Silurian periods based on clumped isotope palaeothermometry and $\delta^{18}O_{apatite}$. The results are comparable to those derived from $\delta^{18}O_{brach}$ and $\delta^{18}O_{bulk}$ values by Brenchley et al. (2003). Our $\delta^{18}O_{brach}$ dataset suggests a steady cooling trend for the Middle Ordovician which is nearly consistent with the trends proposed by Grossman and Joachimski, (2020) and Trotter et al. (2008). Following the relatively warm late Katian, an abrupt worldwide climate cooling in the Hirnantian is obvious in all comparative studies (Fig. 8; Trotter et al., 2008; Grossman and Joachimski, 2020; Männik et al., 2021). The Ordovician and Silurian brachiopod temperature records agree with the temperatures recorded from conodont apatite, considering the low-temperature values representing the Hirnantian and early Silurian. The early Silurian temperature values from this study and from Grossman and Joachimski, (2020) are nearly consistent with the Middle to Late Ordovician ranges, except for the Rhuddanian temperature values reflecting climatic instability before the return to equatorial temperatures comparable to the present in the Wenlock (Fig. 8).

The absolute temperature values calculated from our data may not be precise but the observed trends are in a good agreement with generally accepted temperature and climatic scenarios. For analysing finer-scale climatic variability through the Ordovician-Silurian interval, much better sampling resolution would be required for several intervals.

CONCLUSIONS

The present study assesses Ordovician-Silurian brachiopod stable isotopic data and focusses on the climatic and environmental changes during these periods in the Baltoscandian palaeobasin. Several major $\delta^{13}C_{brac}$ excursions identified in the Ordovician-Silurian in the Estonian Shelf are consistent with previously documented excursions in bulk carbonate stable isotopic curves. The oxygen isotope composition of fossil brachiopods shows a general secular trend from the Early to Late Ordovician towards heavier $\delta^{18}O$ values The Baltoscandian $\delta^{18}O_{brac}$ data suggest warmer temperatures during the Early Ordovician (Floian) and a cooling trend towards the Middle Ordovician, which agrees with the oxygen isotopic data from conodont phosphate, as well as with the results of previous isotope studies in Laurentia and other palaeocontinents. The Hirnantian glaciation HICE episode corresponds to a minimum temperature. The post-HICE data suggest a rising temperature trend. Another temperature minimum is evident in the strata reflecting the Ireviken Event, correlated with the Jaani Regional Stage in Estonia. The absolute temperature values calculated from our data may not be precise but the trends observed are largely parallel to known global temperature and climatic trends despite the plate tectonic drift of Baltica from higher southern palaeolatitudes to the tropical realm during this period. The results also show that the carbon and oxygen stable isotopic composition of Paleozoic brachiopods can tentatively be used for palaeoenvironmental interpretation.

Supplementary online data. Supplementary material online can be found at https://dx.doi.org/10.23673/re-351. It contains the list of brachiopod samples, together with analytical results (stable carbon and oxygen isotope ratios).

Acknowledgements. This publication was financially supported by the projects PRG836 (Tracing the origins of early Paleozoic stable carbon isotope excursions – global, regional and local drivers) and PRG 1701 (From Greenhouse to Icehouse: Reconstructing Ordovician Climate Transitions and Biotic Responses in Baltica) from the Estonian Research Agency and Ministry of Education and Research, and additionally by the Institute of Ecology and Earth Sciences, University of Tartu. This is a contribution to the IGCP 653 (The onset of the Great Ordovician Biodiversification Event) and 735 [Rocks and the Rise of Ordovician Life (Rocks n' ROL)].

REFERENCES

Ainsaar, L., Kaljo, D., Martma, T., Meidla, T., Männik, P., Nõlvak, J., Tinn, O., 2010. Middle and Upper Ordovician carbon isotope chemostratigraphy in Baltoscandia: a correlation standard and clues to environmental history. Palaeogeography, Palaeoclimatology, Palaeoecology, **294**: 189–201. https://doi.org/10.1016/j.palaeo.2010.01.003

Ainsaar, L., Truumees, J., Meidla, T., 2015. The position of the Ordovician–Silurian boundary in Estonia tested by high-resolution $\delta^{13}C$ chemostratigraphic correlation. In: Chemostratigraphy (ed. M. Ramkumar): 395–412. Elsevier. https://doi.org/10.1016/B978-0-12-419968-2.00015-7

Ainsaar, L., Tinn, O., Dronov, A., Kiipli, E., Radzevičius, S., Meidla, T., 2020. Stratigraphy and facies differences of the Middle Darriwilian isotopic carbon excursion (MDICE) in Baltoscandia. Estonian Journal of Earth Sciences, **69**: 214–222. https://doi.org/10.3176/earth.2020.16

Azmy, K., Veizer, J., Bassett, M.G., Copper, P., 1998. Oxygen and carbon isotopic composition of Silurian brachiopods: implications for coeval seawater and glaciations. GSA Bulletin, **110**: 1499–1512. https://doi.org/10.1130/0016-7606(1998)110<1499:OACICO>2.3.CO;2

Bartlett, R., Elrick, M., Wheeley, J.R., Polyak, V., Desrochers, A., Asmerom, Y., 2018. Abrupt global-ocean anoxia during the Late Ordovician–early Silurian detected using uranium isotopes of marine carbonates. Proceedings of the National Academy of Sciences, **115**: 5896–5901. https://doi.org/10.1073/pnas.1802438115

Bergström, S.M., Schmitz, B., Saltzman, M.R., Huff, W.D., Finney, S., Berry, W., 2010. The Upper Ordovician Guttenberg $\delta^{13}C$ excursion (GICE) in North America and Baltoscandia: occurrence, chronostratigraphic significance, and paleoenvironmental relationships. GSA Special Papers, **466**: 37–67. https://dx.doi.org/10.1130/2010.2466(04)

Bond, D.P., Grasby, S.E., 2020. Late Ordovician mass extinction caused by volcanism, warming, and anoxia, not cooling and glaciation. Geology, **48:** 777–781. https://doi.org/10.1130/G47377.1

Brand, U., Veizer, J., 1980. Chemical diagenesis of a multicomponent carbonate system; 1, Trace elements. Journal of Sedimentary Research, **50**: 1219–1236. https://doi.org/10.1306/212F7BB7-2B24-11D7-8648000102C1865D

Brand, U., Bitner, M.A., Logan, A., Azmy, K., Crippa, G., Angiolini, L., Colin, P., Griesshaber, E., Harper, E.M., Ruggiero, E.T., 2019. Brachiopod-based oxygen-isotope thermometer: update and review. Rivista Italiana di Paleontologia e Stratigrafia, **125**: 3. https://dx.doi.org/10.13130/2039-4942/12226

Brenchley, P.J., Marshall, J.D., Carden, G.A.F., Robertson, D.B.R., Long, D.G.F., Meidla, T., Hints, L., Anderson, T.F., 1994. Bathymetric and isotopic evidence for a short-lived late Ordovician glaciation in a greenhouse period. Geology, **22**: 295–298. https://doi.org/10.1130/0091-7613(1994)022<0295:BAIEFA>2.3.CO;2.

Brenchley, P.J., Marshall, J., Underwood, C.J., 2001. Do all mass extinctions represent an ecological crisis? Evidence from the Late Ordovician. Geological Journal, **36**: 329–340. https://doi.org/10.1002/gj.880

Brenchley, P.J., Carden, G., Hints, L., Kaljo, D., Marshall, J., Martma, T., Meidla, T., Nõlvak, J., 2003. High-resolution stable isotope stratigraphy of Upper Ordovician sequences: constraints on the timing of bioevents and environmental changes associated with mass extinction and glaciation. GSA Bulletin, **115**: 89–104 https://doi.org/10.1130/0016-7606(2003)115<0089:HRSISO>2.0.CO;2

Buggisch, W., Joachimski, M.M., Lehnert, O., Bergström, S.M., Repetski, J.E., Webers, G.F., 2010. Did intense volcanism trigger the first Late Ordovician icehouse? Geology, **38**: 327–330. https://doi.org/10.1130/G30577.1

Chen, X., Rong, J., Fan, J., Zhan, R., Mitchell, C.E., Harper, D.A., Melchin, M.J., Peng, A., Finney, S.C., Wang, X., 2006. The Global Boundary Stratotype Section and Point (GSSP) for the base of the Hirnantian Stage (the uppermost of the Ordovician System). Episodes, **29**: 183. https://doi.org/10.18814/epiiugs/2006/v29i3/004

Cocks, L.R.M., Torsvik, T.H., 2005. Baltica from the late Precambrian to mid-Paleozoic times: the gain and loss of a terrane's identity. Earth-Science Reviews, **72**: 39–66. https://doi.org/10.1016/j.earscirev.2005.04.001

Dronov, A., Rozhnov, S., 2007. Climatic changes in the Baltoscandian basin during the Ordovician: sedimentological and palaeontological aspects. Acta Palaeontologica Sinica, **46**: 108.

Edward, O., Korte, C., Ullmann, C.V., Colmenar, J., Thibault, N., Bagnoli, G., Stouge, S., Rasmussen, C.M., 2022. A Baltic perspective on the Early to Early Late Ordovician $\delta^{13}C$ and $\delta^{18}O$ records and its paleoenvironmental significance. Paleoceanography and Paleoclimatology, **37**: e2021PA004309. https://doi.org/10.1029/2021PA004309

Edwards, C.T., Saltzman, M.R., 2014. Carbon isotope ($\delta^{13}C_{carb}$) stratigraphy of the Lower–Middle Ordovician (Tremadocian–Darriwilian) in the Great Basin, western United States: implications for global correlation. Palaeogeography, Palaeoclimatology, Palaeoecology, **399**: 1–20. http://dx.doi.org/10.1016/j.palaeo.2014.02.005

Epstein, S., Buchsbaum, R., Lowenstam, H., Urey, H.C., 1951. Carbonate-water isotopic temperature scale. GSA Bulletin, **62**: 417–426. https://doi.org/10.1130/0016-7606(1951)62[417:CITS]2.0.CO;2

Finnegan, S., Bergmann, K., Eiler, J.M., Jones, D.S., Fike, D.A., Eisenman, I., Hughes, N.C., Tripati, A.K., Fischer, W.W., 2011. The magnitude and duration of Late Ordovician–Early Silurian glaciation. Science, **331**: 903–906. https://doi.org/10.1126/science.1200803

Goldman, D., Sadler, P.M., Leslie, S.A., 2020. Chapter 20. The Ordovician Period. In: Geologic Time Scale 2020 (eds. F.M. Gradstein, J.G. Ogg, M.D. Schmitz and G.M. Ogg): 631–694. Elsevier. https://doi.org/10.1016/B978-0-12-824360-2.00020-6

Gorjan, P., Kaiho, K., Fike, D.A., Xu, C., 2012. Carbon-and sulfur-isotope geochemistry of the Hirnantian (Late Ordovician) Wangjiawan (Riverside) section, South China: Global correlation and environmental event interpretation. Palaeogeography, Palaeoclimatology, Palaeoecology, **337**: 14–22. https://doi:10.1016/j.palaeo.2012.03.021

Gradstein, F.M., Ogg, J.G., Schmitz, M.D., Ogg, G.M., 2020. Geologic Time Scale 2020. Elsevier. https://doi.org/10.1016/B978-0-12-824360-2.00002-6

Grossman, E.L., 2012. Applying oxygen isotope paleothermometry in deep time. The Paleontological Society Papers, **18**: 39–68. https://doi.org/10.1017/S1089332600002540

Grossman, E., Joachimski, M., 2020. Oxygen isotope stratigraphy. In: Geologic Time Scale 2020 (eds. F.M. Gradstein, J.G. Ogg, M.D. Schmitz and G.M. Ogg): 279–307. Elsevier. https://doi.org/10.1016/B978-0-12-824360-2.00010-3

Gul, B., Ainsaar, L., Meidla, T., 2021. Latest Ordovician-early Silurian palaeoenvironmental changes and palaeotemperature trends indicated by stable carbon and oxygen isotopes from northern Estonia. Estonian Journal of Earth Sciences, **70**: 196–209. https://doi.org/10.3176/earth.2021.14

Hammarlund, E.U., Dahl, T.W., Harper, D.A., Bond, D.P., Nielsen, A.T., Bjerrum, C.J., Schovsbo, N.H., Schönlaub, H.P., Zalasiewicz, J.A., Canfield, D.E., 2012. A sulfidic driver for the end-Ordovician mass extinction. Earth and Planetary Science Letters, **331**: 128–139. https://doi.org/10.1016/j.epsl.2012.02.024

Harris, M.T., Sheehan, M., Ainsaar, L., Hints, L., Männik, P., Nõlvak, J., Rubel, M., 2004. Upper Ordovician sequences of western Estonia. Palaeogeography, Palaeoclimatology, Palaeoecology, **210**: 135–148. https://doi.org/10.1016/j.palaeo.2004.02.045

Heath, R.J., Brenchley, J., Marshall, J.D., 1998. Early Silurian carbon and oxygen stable-isotope stratigraphy of Estonia: implications for climate change: Silurian cycles – linkages of dynamic stratigraphy with atmospheric, oceanic and tectonic changes. New York State Museum Bulletin, **491**: 313–327.

Hints, L., Hints, O., Kaljo, D., Kiipli, T., Männik, P., Nõlvak, J., Pärnaste, H., 2010. Hirnantian (latest Ordovician) bio-and chemostratigraphy of the Stirnas-18 core, western Latvia. Estonian Journal of Earth Sciences, **59**: 1–24. https://doi.org/10.3176/earth.2010.1.01

Hints, O., Ainsaar, L., Lepland, A., Liiv, M., Männik, P., Meidla, T., Nõlvak, J., Radzevičius, S., 2023. Paired carbon isotope chemostratigraphy across the Ordovician–Silurian boundary in central East Baltic: regional and global signatures. Palaeogeography, Palaeoclimatology, Palaeoecology, **624**: 111640. https://doi.org/10.1016/j.palaeo.2023.111640

Immenhauser, A., Kenter, J.A., Ganssen, G., Bahamonde, J.R., Van Vliet, A., Saher, M.H., 2002. Origin and significance of isotope shifts in Pennsylvanian carbonates (Asturias, NW Spain). Journal of Sedimentary Research, **72**: 82–94. https://doi.org/10.1306/051701720082

Jacobsen, S.B., Kaufman, A.J., 1999. The Sr, C and O isotopicevolution of Neoproterozoic seawater. Chemical Geology, **161:** 37–57. https://doi.org/10.1016/S0009-2541(99)00080-7

Kaljo, D., Hints, L., Martma, T., Nõlvak, J., 2001. Carbon isotope stratigraphy in the latest Ordovician of Estonia. Chemical Geology, **175**: 49–59. https://doi.org/10.1016/S0009-2541(00)00363-6

Kaljo, D., Martma, T., Saadre, T., 2007. Post-Hunnebergian Ordovician carbon isotope trend in Baltoscandia, its environmental implications and some similarities with that of Nevada. Palaeogeography, Palaeoclimatology, Palaeoecology, **245**: 138–155. https://doi.org/10.1016/j.palaeo.2006.02.020

Kaljo, D., Hints, L., Martma, T., Nõlvak, J., 2017. A multiproxy study of the Puhmu core section (Estonia, Upper Ordovician): consequences for stratigraphy and environmental interpretation. Estonian Journal of Earth Sciences, **66**: 77–92. https://doi.org/10.3176/earth.2017.08

Lehnert, O., Männik, P., Joachimski, M.M., Calner, M., Frýda, J., 2010. Palaeoclimate perturbations before the Sheinwoodian glaciation: a trigger for extinctions during the 'Ireviken Event'. Palaeogeography, Palaeoclimatology, Palaeoecology, **296**: 320–331. https://doi.org/10.1016/j.palaeo.2010.01.009

Ling, H.-F., Feng, H.-Z., Pan, J.-Y., Jiang, S.-Y., Chen, Y.-Q., Chen, X., 2007. Carbon isotope variation through the Neoproterozoic Doushantuo and Dengying Formations, South China: implications for chemostratigraphy and paleoenvironmental change. Palaeogeography, Palaeoclimatology, Palaeoecology, **254**: 158–174. https://doi.org/10.1016/j.palaeo.2007.03.023

Männik, P., 2014. The Silurian System in Estonia. 4th Annual Meeting of IGCP 591 (eds. H. Bauert, O. Hints, T. Meidla and P. Männik): 123–128. Estonia, 10–19 June 2014. Abstracts and Field Guide. University of Tartu, Tartu.

Männik, P., Loydell, D.K., Nestor, V., Nõlvak, J., 2015. Integrated Upper Ordovician–lower Silurian biostratigraphy of the Grötlingbo-1 core section, Sweden. GFF, **137:** 226–244. https://doi.org/10.1080/11035897.2015.1042032

Männik, P., Lehnert, O., Nõlvak, J., Joachimski, M.M., 2021. Climate changes in the pre-Hirnantian Late Ordovician based on $\delta^{18}O_{phos}$ studies from Estonia. Palaeogeography, Palaeoclimatology, Palaeoecology, **569**: 110347. https://doi.org/10.1016/j.palaeo.2021.110347

Melchin, M.J., Holmden, C.E., 2006. Carbon isotope chemostratigraphy of the Llandovery in Arctic Canada: implications for global correlation and sea-level change. GFF **128**: 173–180. https://doi.org/10.1080/11035890601282173

Meidla, T., Ainsaar, L., Hints, O., 2014. The Ordovician System in Estonia. 4th Annual Meeting of IGCP 591 (eds. H. Bauert, O. Hints, T. Meidla and P. Männik): 116–122. Estonia, 10–19 June 2014. Abstracts and Field Guide. University of Tartu, Tartu.

Meidla, T., Truuver, K., Tinn, O., Ainsaar, L., 2020. Ostracods of the Ordovician–Silurian boundary beds: Jūrmala core (Latvia) and its implications for Baltic stratigraphy. Estonian Journal of Earth Sciences, **69**: 233–247. https://doi.org/10.3176/earth.2020.20

Meidla, T., Ainsaar, L., Hints, O., Radzevičius, S., 2023. Ordovician of the Eastern Baltic palaeobasin and the Tornquist Sea margin of Baltica. Geological Society Special Publications, **532:** 317-343. https://doi.org/10.1144/SP532-2022-14

Munnecke, A., Calner, M., Harper, D.A., Servais, T., 2010. Ordovician and Silurian sea-water chemistry, sea level, and climate: a synopsis. Palaeogeography, Palaeoclimatology, Palaeoecology, **296**: 389–413. https://doi.org/10.1016/j.palaeo.2010.08.001

Nestor, H., Einasto, R., 1997. Ordovician and Silurian carbonate sedimentation basin. In: Geology and Mineral Resources of Estonia (eds. A. Raukas and A. Teedumäe): 192–204. Estonian Academy Publishers, Tallinn.

Quinton, P.C., Law, S., MacLeod, K.G., Herrmann, A.D., Haynes, J.T., Leslie, S.A., 2018. Testing the early Late Ordovician coolwater hypothesis with oxygen isotopes from conodont apatite. Geological Magazine, **155**: 1727–1741. https://doi.org/10.1017/S0016756817000589

Rasmussen, C.M.O., Ullmann, C.V., Jakobsen, K.G., Lindskog, A., Hansen, J., Hansen, T., Eriksson, M.E., Dronov, A., Frei, R., Korte, C., Nielsen, A.T., Harper, D.A.T., 2016. Onset of main Phanerozoic marine radiation sparked by emerging Mid Ordovician icehouse. Scientific Reports, **6**: 1–9. https://doi.org/10.1038/srep18884

Rong, J., Melchin, M., Williams, S.H., Koren, T.N., Verniers, J., 2008. Report of the restudy of the defined global stratotype of the base of the Silurian System. Episodes, **31**: 315–318. https://doi.org/10.18814/epiiugs/2008/v31i3/005

Rosenau, N.A., Herrmann, A.D., Leslie, S.A., 2012. Conodont apatite $\delta^{18}O$ values from a platform margin setting, Oklahoma, USA: implications for initiation of Late Ordovician icehouse conditions. Palaeogeography, Palaeoclimatology, Palaeoecology, **315**: 172–180. https://doi.org/10.1016/j.palaeo.2011.12.003

Saltzman, M.R., Young, S.A., 2005. Long-lived glaciation in the Late Ordovician? Isotopic and sequence-stratigraphic evidence from western Laurentia. Geology, **33**: 109–112. https://doi.org/10.1130/G21219.1

Sheehan, M., 2001. The late Ordovician mass extinction. Annual Review of Earth and Planetary Sciences, **29**: 331–364. https://doi.org/10.1146/annurev.earth.29.1.331

Shields, G.A., Carden, G.A., Veizer, J., Meidla, T., Rong, J.-Y., Li, R.-Y., 2003. Sr, C, and O isotope geochemistry of Ordovician brachiopods: a major isotopic event around the Middle-Late Ordovician transition. Geochimica et Cosmochimica Acta, **67**: 2005–2025. https://doi.org/10.1016/S0016-7037(02)01116-X

Swart, K.J.S., 2015. The geochemistry of carbonate diagenesis. The past, present and future. Sedimentology**, 62**: 1233–1304. https://doi.org/10.1111/sed.12205

Trotter, J.A., Williams, I.S., Barnes, C.R., Lécuyer, C., Nicoll, R.S., 2008. Did cooling oceans trigger Ordovician biodiversification? Evidence from conodont thermometry. Science, **321**: 550–554. https://doi.org/10.1126/science.1155814

Trotter, J.A., Williams, I.S., Barnes, C.R., Männik, P., Simpson, A., 2016. New conodont $\delta^{18}O$ records of Silurian climate change: implications for environmental and biological events.

Palaeogeography, Palaeoclimatology, Palaeoecology, **443**: 34–48. https://doi.org/10.1016/j.palaeo.2015.11.011

Torsvik, T.H., Cocks, L.R.M., 2016. Earth History and Palaeogeography. Cambridge University Press. https://dx.doi.org/10.1017/9781316225523

Urey, H.C., 1947. The thermodynamic properties of isotopic substances. Journal of the Chemical Society: 562–581. https://doi.org/10.1039/jr9470000562

Veizer, J., Ala, D., Azmy, K., Bruckschen, P., Buhl, D., Bruhn, F., Carden, G. A., Diener, A., Ebneth, S., Godderis, Y., 1999. $^{87}Sr/^{86}Sr$, $\delta^{13}C$ and $\delta^{18}O$ evolution of Phanerozoic seawater. Chemical Geology, **161**: 59–88. https://doi.org/10.1016/S0009-2541(99)00081-9

Zhang, J., Lyons, T.W., Li, C., Fang, X., Chen, Q., Botting, J., Zhang, Y., 2022. What triggered the Late Ordovician mass extinction (LOME)? Perspectives from geobiology and biogeochemical modeling. Global and Planetary Change, **216**: 103917. https://doi.org/10.1016/j.gloplacha.2022.103917